Journal of Mechanics in Medicine and Biology
Vol. 5, No. 1 (2005) 105–121

World Scientific
www.worldscientific.com

TOWARDS COMPUTING BRAIN DEFORMATIONS FOR DIAGNOSIS, PROGNOSIS AND NEUROSURGICAL SIMULATION

KAROL MILLER*,‡,§, ZEIKE TAYLOR§ and WIESLAW L. NOWINSKI†,‡

‡*Biomedical Imaging Lab.*
Agency for Science Technology and Research
30 Biopolis Street, HO Matrix, Singapore 138671

§*School of Mechanical and Materials Engineering*
The University of Western Australia
35 Stirling Highway, Crawley/Perth WA 6009, Australia
**kmiller@mecn.uwa.edu.au*
†*wieslaw@bii.a-star.edu.sg*

The objective of our research is to create a system computing brain deformations. We have in view both clinical and training applications, such as "brain shift" calculation, prognosis and diagnosis of development of brain diseases as well as surgical simulators for planning and education. In this paper, we specifically address issues related to creating geometrically and mechanically precise representations of the brain. The method comprises of the following steps: (1) development of a 3D anatomical brain atlas, (2) construction of a finite element mesh of the atlas, (3) creation of a mathematical model, and (4) development of an efficient computational model. We discuss two types of approaches to model deformation behavior of the brain: single-phase brain tissue model, suitable for analysis of relatively short events such as surgical actions; and bi-phasic brain tissue model, well suited for calculations leading to prognosis of the development of diseases. As an illustration of the presented concepts we provide examples of 3D meshing, calculation of reaction force acting on a surgical tool using a single-phase mathematical model, and calculations of the development of hydrocephalus and the effects of tumor growth using the bi-phasic modeling approach.

Keywords: Computer-integrated medicine; brain atlas; brain tissue; mathematical modeling; neurosurgery simulation.

1. Introduction

Effective diagnosis and treatment requires integration of numerous sensing modalities. This will become particularly important in the operating room of the future.[1] The key sensing modality used in today's clinical practice as well as in computer-aided surgery and diagnosis is vision. Similarly important in treatment is touch, which remains underestimated and underutilized in computer-aided solutions. The importance of mechanics (i.e. force and tactile feedback) in computer simulation for medicine is growing. Certain aspects of it have already found their way into popular accounts.[2]

To achieve a realistic, clinically acceptable computer simulation one requires an adequate model, capturing the intrinsic physical properties of the organ considered, intervention performed, and surgical accessories used. Neurosurgery is particularly demanding as the brain is the most complicated object in the known universe. Modeling of physical properties of the brain is still an uncovered area pioneered by only a few.[3–5]

The physics-based model should contain detailed anatomical (geometrical) information. Such information can be provided by a suitable electronic brain atlas, e.g. the Cerefy Brain Atlas.[6] In the case of patient-specific applications, geometric information provided by the atlas has to be individualized (through an appropriate registration process, not discussed in this paper) to fit to a particular individual. Next, a computational grid has to be created on the domain of interest. In most practical cases, this amounts to producing a finite element mesh. Mathematical models governing the deformation behavior of continua consist of sets of partial differential equations supplemented by constitutive relations, boundary and initial conditions. Numerical methods are needed to solve such sets of equations. These methods require appropriate discretization of the domain of interest. The most common and probably the most effective numerical method for sets of partial differential equations is the finite element method.[7] After creating the mesh, the partial differential equations of a chosen mathematical model are solved and the evolution of variables of interest obtained.

The objective of our research is to create a system computing brain deformations, Fig. 1, and to introduce a framework for the development of physics-based applications.

In this paper we focus on two aspects of the system pictured in Fig. 1:

(i) using an electronic brain atlas to obtain geometric information about the brain and meshing; and
(ii) selection of mathematical model for applications with different characteristic time scales and strain rates.

2. Electronic Brain Atlases as a Source of Anatomic and Geometric Information for Mathematical Models of the Brain

The Cerefy brain atlas database has been developed and introduced to clinical, research, and educational practice,[6,8,9] Fig. 2. This database contains multiple, complementary brain atlases with gross anatomy, brain connections, subcortical structures, and sulcal patterns. For the purpose of this work, the Talairach–Tournoux (TT) brain atlas containing gross anatomy is used.[10] In order to construct a computerized version of the TT atlas, the print atlas plates were digitized with high resolution and the digitized plates were extensively preprocessed, enhanced, and extended.[8,9,11] The electronic atlas images were fully segmented and labeled with subcortical structures and cortical regions including Brodmann's areas.

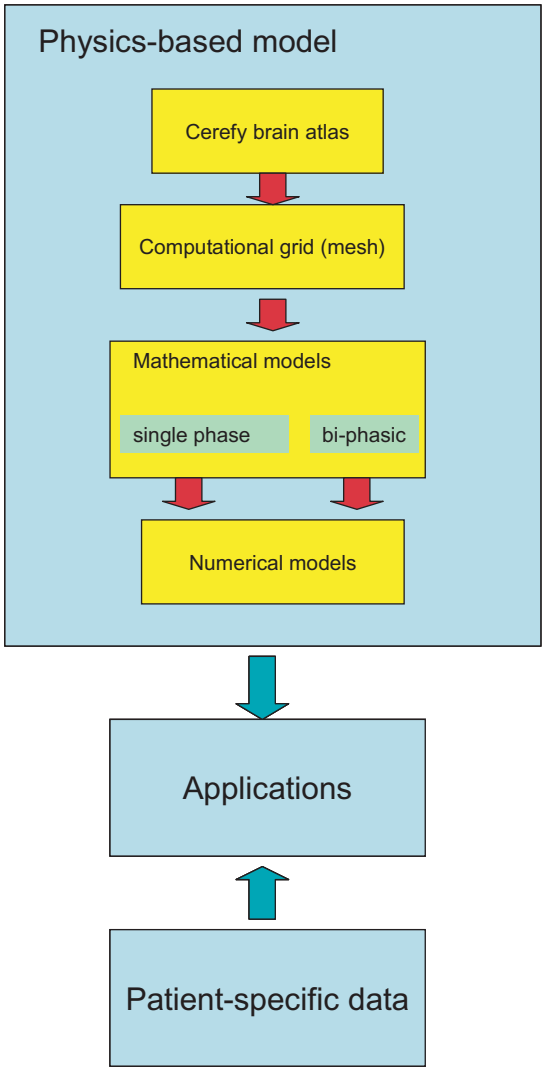

Fig. 1. Framework for developing physics-based neuro applications.

Three-dimensional (3D) polygonal models of the subcortical structures and Brodmann's areas were also constructed.

The brain atlas is used in several applications for neurosurgery, neuroradiology, human brain mapping, and education. Two applications, NeuroPlanner[12] and BrainBench,[13] demonstrate the potential of the brain atlas in neurosurgery planning and are suitable candidates for integrating results from this research.

In order to use in computations anatomical and geometric information contained within the electronic brain atlas suitable grids (meshes) have to be developed. In

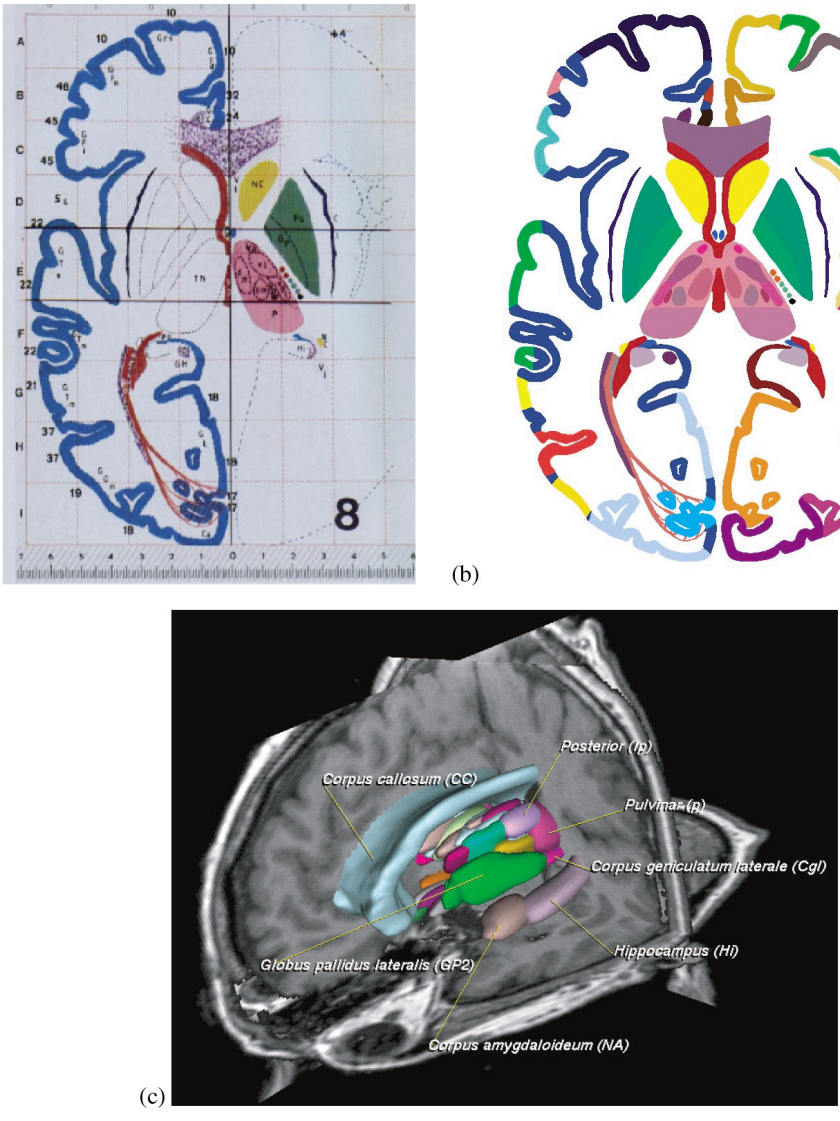

Fig. 2. Cerefy brain atlas: (a) original print image; (b) electronic image, segmented and color-coded; and (c) 3D models superimposed on patient-specific data.

our implementation,[14–16] meshing is done in two automatic stages: 2D and 3D meshing.

In 2D meshing, the segmented structure of interest is subdivided into quadrilateral elements. To perform discretization, a grid-based approach is used.[17] In our experience, this method is most suited for meshing complex anatomical shapes. A grid of parallel lines of variable distance is overlaid on the structure dividing its

interior into quadrilateral planar elements. The boundary elements are generated from the intersection of the boundary with the grid lines.

3D meshes are constructed subsequently by connecting corresponding nodes at adjacent grid planes. Two adjacent 2D elements are linked together to generate one hexahedral (eight-node) 3D element. Finally, optimization is performed to standardize the elements to conform to FE analysis requirements. The procedure checks the quality of elements by computing their Jacobians, aspect ratios, volumes and areas.

The process of mesh generation is illustrated in Fig. 3. An ongoing effort is to extend this work for 3D meshing of the Cerefy brain atlas.

3. Approaches to Modeling Brain Deformation Behavior

The brain is the most complex organ. Its main structures include the cerebral hemispheres, the diencephalon, the brain stem and the cerebellum. The cerebral hemispheres consist of the outer layer of grey matter and the inner core of white matter. The grey matter consists of nerve cell bodies and nerve fibers not surrounded by the myelin. The white matter consists of bundles of long nerve fibers surrounded by myelin sheath. This gives the tissue its white appearance and distinguishes it from the grey matter. In humans, approximately 40% of the brain is composed of the white matter.[18] The brain is maintained in place by membranes and the meninges. They consist of connective tissues containing collagen and other elastic fibers. The brain is also protected by the cerebrospinal fluid.

3.1. *Modeling the brain for surgical simulation*

Despite its complexity the brain, from the perspective of surgical simulation, can be considered a single-phase continuum. The main reason for neglecting effects of interstitial fluid flow within the brain tissue is that the time scale of this flow is much different (larger) to the time scale relevant to surgical procedures. This relevant time scale ranges from tens of seconds to minutes.

The mathematical model of the deformation behavior of a single-phase continuum consists of the standard solid-mechanical partial differential equations of equilibrium (or dynamics), boundary and initial conditions, and a constitutive model for the brain tissue.

Depending on whether one decides to measure stresses and strains with respect to the deformed or undeformed configuration, different (but equivalent) formulations of equations of equilibrium should be used.[19] If Cauchy stress and Almansi strain, both measured with respect to the deformed (current) configuration, have been chosen the equation of equilibrium can be written in the following way:

$$\boldsymbol{\tau}^{ij}_{,i} + \rho F_i = 0, \tag{1}$$

where $\boldsymbol{\tau}$ denotes Cauchy stress, ρ is a mass density, F_i is a body force per unit mass in direction i, and the subscript comma indicates covariant differentiation

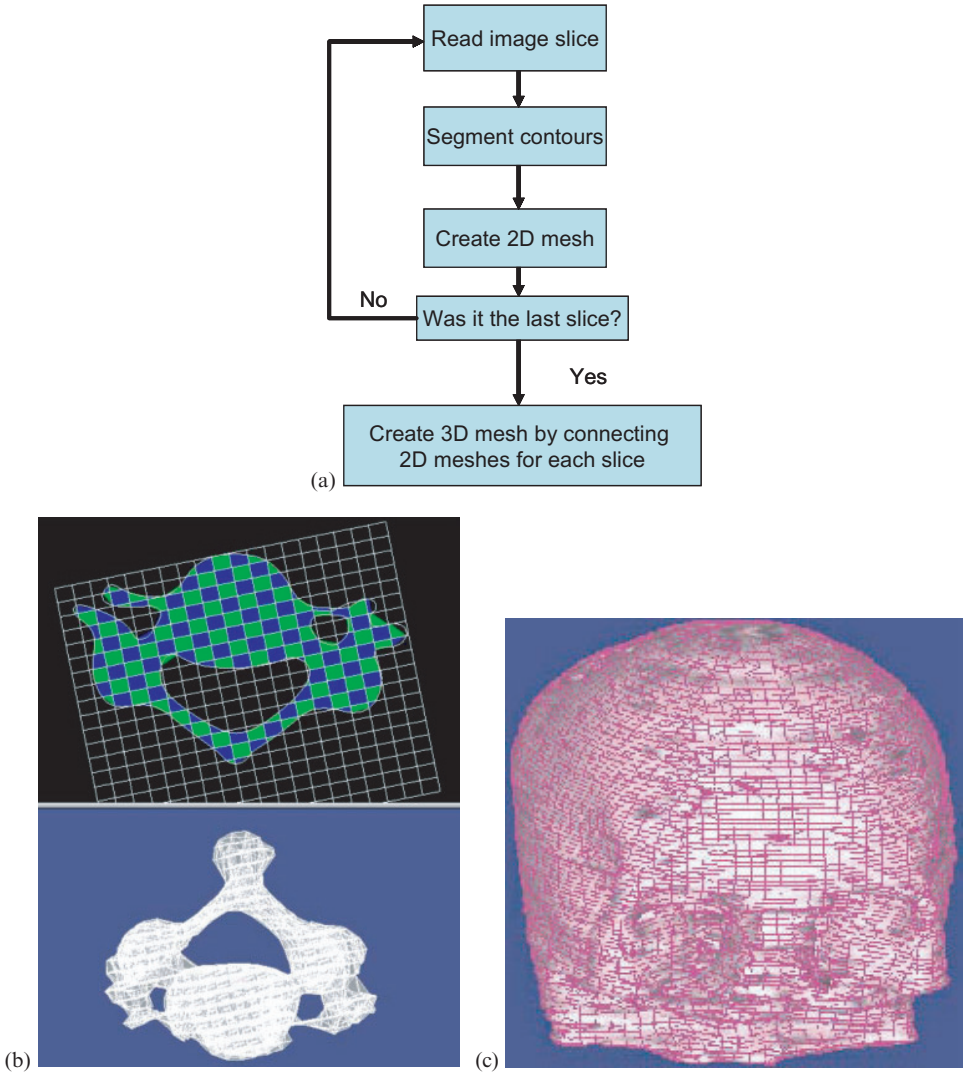

Fig. 3. Stages of mesh generation (a) and examples of 3D meshing: vertebrae[14] (b) and skull (c).

with respect to the deformed configuration. Repeated index summation convention was used.

In the case where Second Piola–Kirchoff stress tensor and Green strain (both measured with respect to undeformed configuration) are preferred, the equations of equilibrium have to be rewritten:

$$\left(\mathbf{S}^{ij} x^{j}_{,k}\right)_{,i} + \rho_0 F_{0_i} = 0, \tag{2}$$

where ρ_0 is a mass density in undeformed configuration and F_{0i} is a body force per unit mass in undeformed configuration in direction i measured with respect to undeformed configuration. Comma denotes covariant differentiation, this time, with respect to the original configuration.

If one prefers Lagrange stress, the equations of equilibrium would look as follows:

$$\mathbf{T}^{ij}_{,i} + \rho_0 F_{0_i} = 0. \tag{3}$$

The formulation of appropriate boundary conditions supplementing the above equations constitutes a significant problem in biomechanics of soft tissues. In the case of the brain, it is possible to assume the rigidity of the skull, certain gap between the brain and the skull, and no friction sliding boundary condition at the skull-brain interface.[20] However, the suggested approach is only a crude approximation. Research on boundary conditions, in the authors' opinion, is at least equally important to the investigation of the mechanical properties of brain internal structures.

In this contribution, we are most interested in the choice of the appropriate constitutive model for the brain tissue. As shown in Fig. 4, the stress-strain behavior of

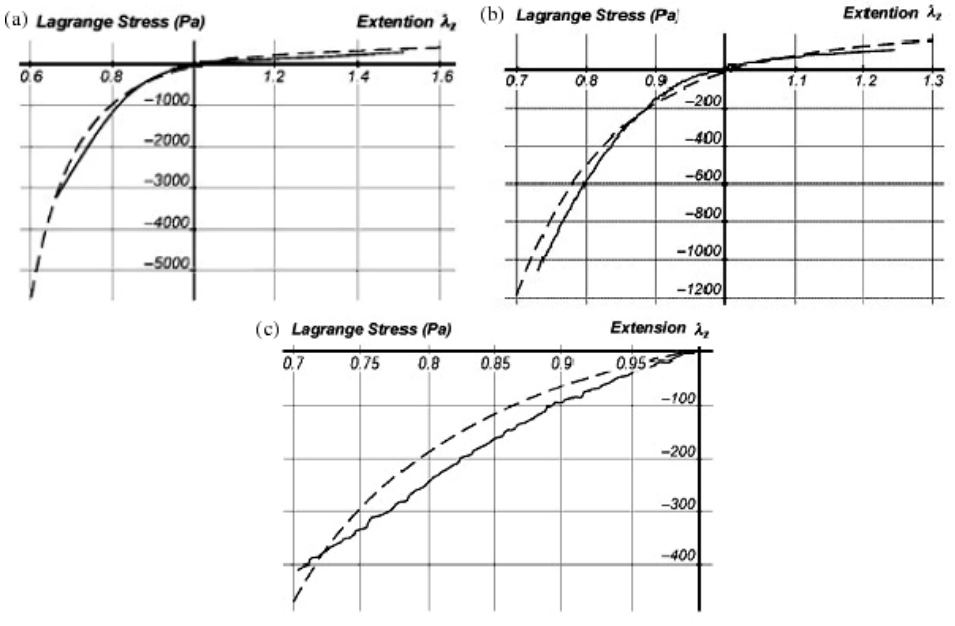

Fig. 4. Experimental (solid line) versus theoretical [dashed line, Eqs. (4) and (5)] results for compression[22] and extension[21] of brain tissue for various loading velocities: (a) loading velocity $= 5.0 \times 10^2\,\mathrm{mm\ min^{-1}}$; corresponding to the strain rate approx. $0.64\,\mathrm{s^{-1}}$, (b) loading velocity $= 5.0\,\mathrm{mm\,min^{-1}}$; corresponding to the strain rate approx. $0.64 \times 10^{-2}\,\mathrm{s^{-1}}$; and (c) loading velocity $= 5.0 \times 10^{-3}\,\mathrm{mm\,min^{-1}}$; corresponding to the strain rate approx. $0.64 \times 10^{-5}\,\mathrm{s^{-1}}$ (compression only).

the brain tissue is non-linear.[21] The stiffness in compression is significantly higher than in extension. One can also observe a strong stress–strain rate dependency. The distinguishing feature of the mathematical model of the brain intended for the simulation of neurosurgery is the strain rate range (the loading speed range) considered — $0.001\,\mathrm{s}^{-1}$–$1.0\,\mathrm{s}^{-1}$ — orders of magnitude lower than that experienced in situations leading to injury and much higher than those encountered in the analysis of brain structural diseases. During loading resulting in such strain rates both non-linear stress–strain and stress–strain rate relations demonstrate their importance.[21,22]

To account for these complexities, we suggest using the following constitutive model[21]:

$$W = \frac{2}{\alpha^2}\int_0 \left[\mu(t-\tau)\frac{d}{d\tau}(\lambda_1^\alpha + \lambda_2^\alpha + \lambda_3^\alpha - 3)\right] d\tau, \tag{4}$$

$$\mu = \mu_0 \left[1 - \sum_{k=1}^{n} g_k\left(1 - e^{-\frac{t}{\tau_k}}\right)\right], \tag{5}$$

where W is a potential function, λ_i's are principal stretches, μ_0 is the instantaneous shear modulus in undeformed state, τ_k are characteristic times, g_k are relaxation coefficients, and α is a material coefficient, which can assume any real value without restrictions. The identified values for the material parameters are given in Table 1.

As can be seen in Fig. 4, the proposed model accounts well for brain tissue behavior in compression and extension for strains up to 30% and strain rates relevant to surgical procedures ($\sim$0.01–$1\,\mathrm{s}^{-1}$).

Such model, as shown in Miller *et al.*[20] can be included in finite element computational model of reaction forces acting on surgical tools. Figure 5 presents the experimental setup and the comparison of the measured and computed forces for the *in vivo* indentation of the swine brain. The forces predicted by our model were about 31% lower than the measured ones. Taking into account the large variability inherent in biological materials, the agreement, in the authors' opinion, is good. The constitutive model used in this study is linear in parameters describing instantaneous response of the material. Therefore, the increase of these parameters by 31% will result in almost perfect reproduction of the experimental force displacement curve.

Table 1. List of material constants for constitutive model of brain tissue, Eqs. (3) and (4), $n = 2$.

Instantaneous response	$k = 1$	$k = 2$
$\mu_0 = 842$ [Pa]; $\alpha = -4.7$	Characteristic time $t1 = .5$ [s]; $g_1 = 0.450$;	Characteristic time $t2 = 50$ [s]; $g_1 = 0.365$;

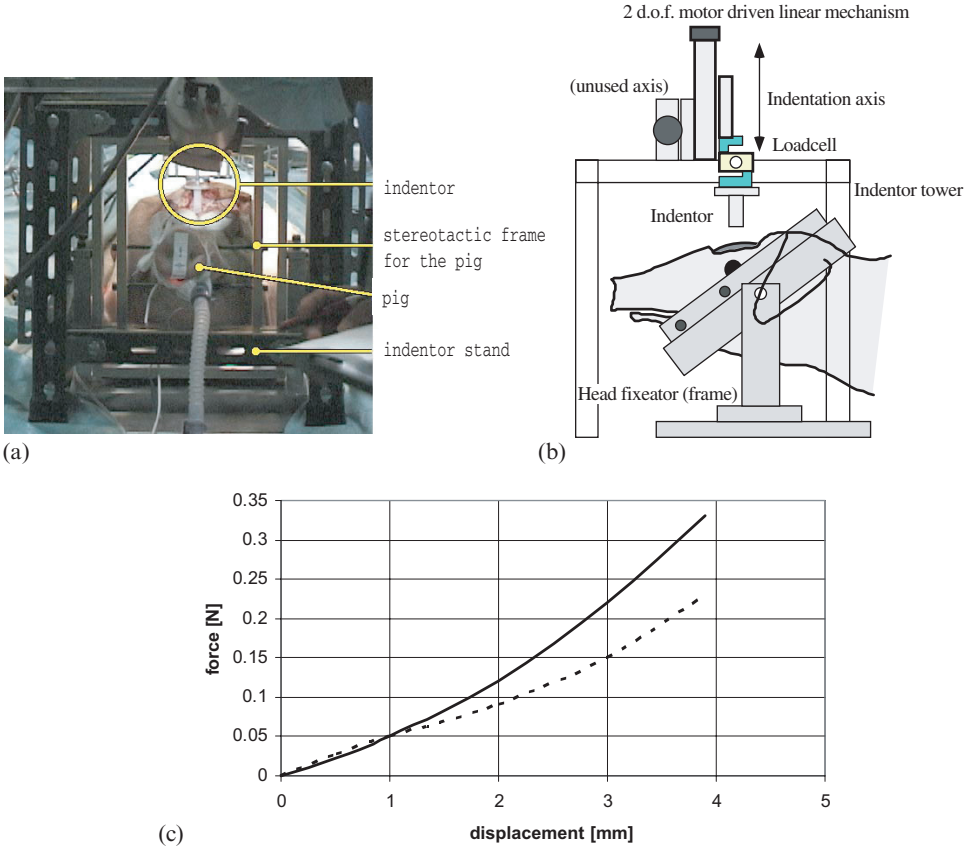

Fig. 5. *In vivo* indentation of swine brain — experiment configuration:[20] (a) swine's head in fixture; (b) schematic of the set-up; and (c) force versus displacement relationship for 1 mm/s indentation speed and 10 mm indenter diameter: solid line — experiment (respiration and heart beat filtered out); dotted line — hyper-viscoelastic analysis results.

3.2. *Modeling the brain for prognosis of structural diseases*

Brain structural diseases, such as hydrocephalus or tumor growth, take from hours to years to develop. Interstitial fluid flow has an important mechanical role to play in such long-lasting phenomena. Since 1980, when the paper by Mow and co-workers[23] initiated the growth of impressive body of knowledge related to modeling mechanical properties of articular cartilage tissues using "bi-phasic theories", the method has acquired a high level of maturity. The non-linear formulations and non-linear finite element models have been developed, and solutions for real life, physiological problems attempted, see papers[24,25] and references cited therein. The automatic schemes have been utilized for model parameter identification.[26,27] The biphasic approach has been also used for modeling of brain tissue mechanical properties.[28,29]

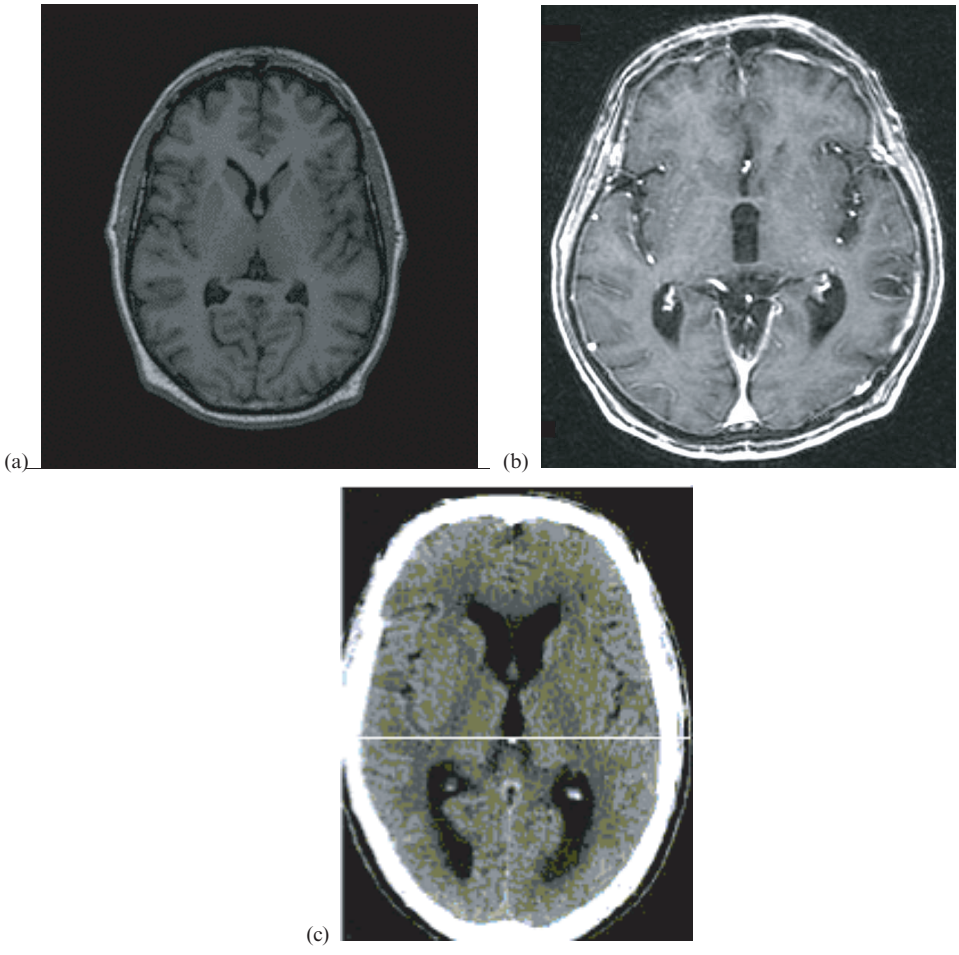

Fig. 6. MR images of (a) normal ventricular configuration; (b) slightly dilated ventricles in a hydrocephalic brain; and (c) CT image of a hydrocephalic brain with significantly dilated ventricles.[35]

The biphasic theory assumes the tissue to be a mixture of two immiscible constituents: a solid deformable porous matrix and a penetrating fluid. Following the work of Nagashima[30] and Peña,[31] the biphasic nature of the brain tissue may be modeled using the principles of Biot's consolidation theory,[31] which was further developed and generalized by Bowen.[32]

3.2.1. *Equilibrium, mass conservation, and fluid flow*

Interstitial fluid flow through the porous medium is modeled using Darcy's law:

$$sn\mathbf{v}_w = -k\frac{\partial \phi}{\partial \mathbf{X}}, \tag{6}$$

where s = saturation, n = porosity, $\mathbf{v}_w$ = wetting liquid velocity with respect to the solid phase, ϕ = pore fluid piezometric head, and k is the permeability of the medium.

Continuity of the liquid phase requires that the rate of increase of fluid mass at a point must be equated with the rate of mass of fluid flowing into this point. For a control volume, V, bounded by the surface, S, this may be stated as:

$$\int_V \frac{1}{J}\frac{d}{dt}(J\rho_w n_w)dV = -\int_S \rho_w n_w \,\mathbf{n}\cdot\mathbf{v}_w dS \tag{7}$$

where J is the ratio of the volume in the current configuration to that of the reference configuration, ρ_w = pore fluid mass density, n_w is the volume ratio of wetting fluid, $\mathbf{n}$ = outward normal vector from the surface, S.

Equilibrium of the medium is achieved by equating internal and external forces:

$$\int_V \tau_c dV = \int_S \mathbf{t} dS + \int sn\rho_w \mathbf{g} dV + \int_V \mathbf{f} dV \tag{8}$$

where τ_c is the Cauchy stress, $\mathbf{t}$ the surface tractions per unit area, $sn\rho_w\mathbf{g}$ the weight of wetting liquid, $\mathbf{g}$ the gravitational acceleration vector, and $\mathbf{f}$ all other external forces.

Again, we are particularly interested in the choice of the constitutive model for the tissue, in this case for a solid phase of the consolidation model. During the development of brain structural diseases the strain-rate is close to zero. It is therefore reasonable to adopt the limiting (hyperelastic) case of the constitutive model given by Eqs. (4) and (5), and Table 1 as a description of the properties of the solid phase:

$$W = \frac{2\mu_\infty}{\alpha^2}(\lambda_1^2 + \lambda_2^2 + \lambda_3^2), \tag{9}$$

where: $\mu_\infty = \sim 155\,\text{Pa}$ is the shear modulus in undeformed state at infinitesimally slow loading. $\alpha = -4.7$.

Permeability, $k = 1.59 \times 10^{-7}\,\text{m/s}$, and Poisson's ratio, $\nu = 0.35$, are obtained from Kaczmarek *et al.*[29] and the initial void ratio for the material is taken as 0.2.[28] Recent work[33] showed no significant difference between white and grey matter elasticity, and so homogeneity and isotropy are assumed for the entire brain.

The fluid phase is considered to be an incompressible, inviscid fluid with mechanical properties as for water.

3.2.2. *Computer simulation of the development of hydrocephalus*

Hydrocephalus is a disorder of the brain associated with disruption to the flow of cerebrospinal fluid (CSF), Fig. 6. CSF is produced by the choroid plexus, within the lateral ventricles of the brain, and under normal conditions is then circulated through the third and fourth ventricles and the spinal cord, and finally absorbed within the sub-arachnoid space.[34] In a hydrocephalic brain, an obstruction may

block this flow and prevent extrusion of CSF from the lateral ventricles. Consequently, ventricular fluid pressure increases and forces expansion of the ventricle walls. Being confined by the rigid skull (except in infantile cases) the periventricular brain parenchyma is compressed, and in acute cases, destroyed. Additionally, significant edema is observed in the periventricular material, particularly in the regions of the frontal and occipital horns, as the increased ventricular pressure forces permeation of the CSF through the surrounding tissue.

Here, we present an example simulation taken from Taylor and Miller.[36] Model geometry was obtained from a horizontal cross-section presented in the anatomic atlas.[10] The section was taken at 20 mm above a reference defined by the anterior and posterior commissures.[10] Pore pressure was fixed at zero at the skull boundary to ensure outward radial CSF flow and drainage in the sub-arachnoid space. The outer brain surface was assumed fixed to the skull and so surface nodes are constrained in all directions. Along the midline boundary, nodes are constrained in the horizontal direction (due to the presence of the left hemisphere), but are allowed to displace vertically. Loading of the ventricular wall was in the form of a distributed fluid pressure over the surface, with a magnitude of 3,000 Pa, in line with previous work.[28,30] Model solutions were obtained using ABAQUS/Standard finite element software.[37] Based on published data,[22] the total development time for hydrocephalus was taken as 4 days (345,600 seconds). Further details can be found in the original publication.[36]

Figure 7 shows the deformed mesh compared with the original configuration. The pressure across the surface of the ventricle produces an overall expansion of the ventricular space. In particular, there is a pronounced lateral displacement of the right wall of the ventricle, and a dilation of the ventricle tips (frontal and occipital horns). Maximal displacement midway along the ventricle right wall is 4.79 mm.

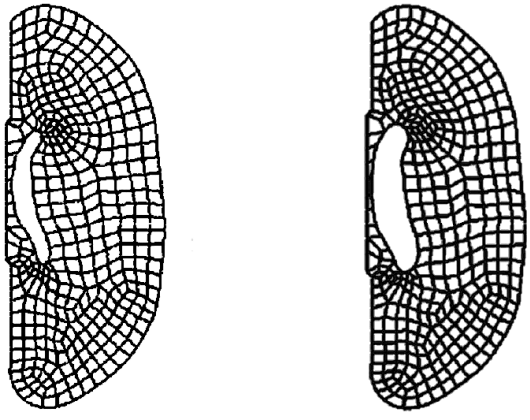

Fig. 7. Comparison of (a) undeformed mesh with (b) deformed model.

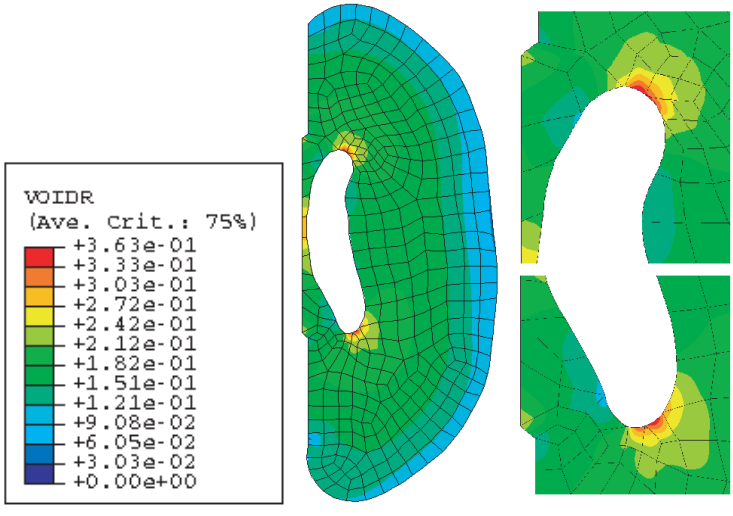

Fig. 8. Void ratio distribution.

Figure 8 shows the void ratio distribution after loading — the unloaded void ratio throughout the medium is 0.2. Significant increases around the ventricular horns are apparent. Void ratios in these regions rise to as much as 0.363.

As the medium remains fully saturated, any increase in void ratio corresponds to an increase in the fluid content in that region. The areas with increased void ratio around the ventricle horns may be identified as areas of fluid edema.

3.2.3. *Computer simulation of the effects of the tumor growth*

Tumor growth can cause a substantial brain deformation and change stress distribution in the tissue as well as patterns of CSF, interstitial fluid and blood flow within the brain. The bi-phasic approach presents itself as an appropriate starting mathematical modeling technique to investigate such phenomena.

Here we present an example simulation. The same geometry as in the simulation of hydrocephalus (see above) was used. The tumor was modeled as a rigid circle of 3 cm diameter. Figure 9 shows the calculated pore pressure distribution within the brain and magnitudes of flow velocity.

Changes of pore pressure and altered patterns of interstitial fluid flow direction and speed may have detrimental effect on brain cell metabolism and function. The ability to predict future changes of field variables characterizing mechanical equilibrium of the brain may lead to improved prognosis and diagnosis methods. For instance, by knowing the tumor growth, it is possible to predict the corresponding intracranial pressure. This information is critical particularly for patients waiting in a queue for their surgery.

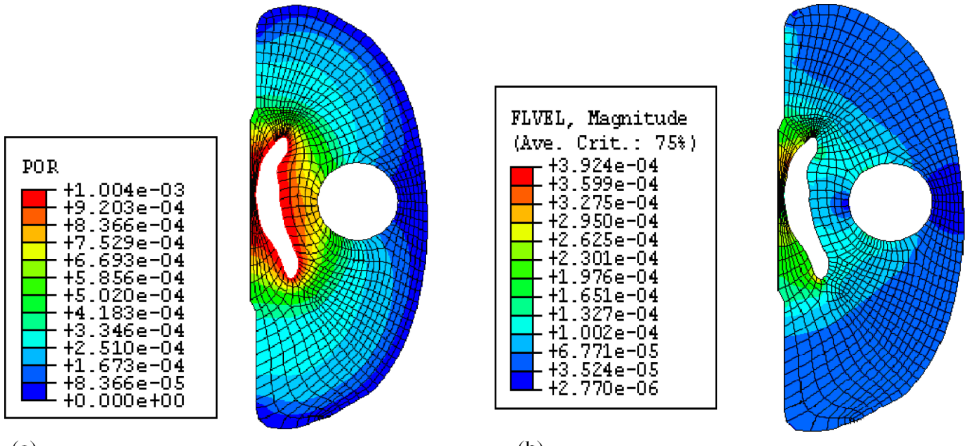

Fig. 9. Results of computer simulation of tumor growth effects on the brain. (a) Pore pressure distribution; (b) magnitude of fluid flow velocity.

4. Discussion, Conclusions and Future Work

Computational biomechanics offers new possibilities for clinical practice as well as medical training. A number of distinct classes of applications can be defined:

(i) clinical applications

- control of surgical robots[3,38]
- intra-operative computations, such as calculation of a "brain shift"
- patient-specific operation planning
- prognosis of the development and effects of diseases

(ii) training applications

- non-patient-specific "average" surgical simulation systems
- simulators for specific applications, such as needle insertion simulators, etc.

In particular we are interested in understanding mechanics of brain biopsy. Appropriate computational models of needle insertion may lead to clinical applications such as recognition of brain structures through measurement of reaction forces acting on the needle as well as to simulators intended for medical training.

To cope with these problems we propose to build a mechanics-based atlas of the human brain. As a starting point for this purpose, we use the Cerefy brain atlas. This anatomical atlas has several advantages, including high parcellation of structures, 3D models, and acceptance by and availability to the clinical community, as it is available in major image guided surgery systems and on stand-alone CD-ROMs.

The choice of the appropriate mathematical model and consequently the appropriate constitutive model for the brain tissue depends on the time-scale and strain-rate range typical for the event one attempts to simulate. As shown in this paper, the preferred model for relatively short events and moderate strain-rates is a single-phase continuum model with hyper-viscoelastic constitutive equation for the tissue. For slow events, one should choose a bi-phasic model with a hyperelastic constitutive equation for the solid phase. This hyperelastc equation is a limiting case for infinitesimally slow strain rates of the more sophisticated hyper-viscoelastic model.

5. Acknowledgments

The financial support of the Australian Research Council (Grant No. DP0343112) and the Biomedical Research Council, Agency for Science, Technology and Research, Singapore is gratefully acknowledged.

References

1. Benabid AL, Nowinski WL, Intraoperative robotics for the practice of neurosurgery: A surgeon's perspective, in Apuzzo ML (ed.), *The Operating Room for the 21th Century*, pp. 103–118, American Association of Neurological Surgeons, Rolling Meadows, 2003.
2. Fox D, Gut Feeling, *New Scientist* 179/2408, pp. 34–37, 2003.
3. Miller K, Chinzei K, Modeling of soft tissues deformation, *J Comp Aid Surg* (Supl., Proc. of Second International Symposium on Computer Aided Surgery, Tokyo Women's Medical College, Shinjuku, Tokyo), pp. 62–63, 1995.
4. Bilston L, Liu Z, Phan-Tiem N, Large strain behaviour of brain tissue in shear: Some experimental data and differential constitutive model, *Biorheology* **38**:335–345, 2001.
5. Prange MT, Margulies SS, Regional, directional, and age-dependent properties of the brain undergoing large deformation, *ASME Journal of Biomechanical Engineering* **124**:244–252, 2002.
6. Nowinski WL, Thirunavuukarasuu A, *The Cerefy Clinical Brain Atlas*, Thieme, New York, 2004.
7. Bathe K-J, *Finite Element Procedures in Engineering Analysis*, Prentice Hall, New Jersey, USA, 1996.
8. Nowinski WL, Computerized brain atlases for surgery of movement disorders, *Seminars in Neurosurgery* **12**(2):183–194, 2001.
9. Nowinski WL, Benabid AL, New directions in atlas-assisted stereotactic functional neurosurgery, in Germano IM (ed.), *Advanced Techniques in Image-Guided Brain and Spine Surgery*, Thieme, New York, pp. 162–174, 2002.
10. Talairach J, Tournoux P, *Co-Planar Stereotaxic Atlas of the Human Brain*, Thieme Medical Publishers, Inc. New York, 1988.
11. Nowinski WL, Fang A, Nguyen BT, Raphel JK, Jagannathan L, Raghavan R, Bryan RN, Miller G, Multiple brain atlas database and atlas-based neuroimaging system, *Computer Aided Surgery* **2**(1):42–66, 1997.
12. Nowinski WL, Yang GY, Yeo TT, Computer-aided stereotactic functional neurosurgery enhanced by the use of the multiple brain atlas database, *IEEE Transactions on Medical Imaging* **19**(1):62–69, 2000.

13. Serra L, Nowinski WL, Poston T, Ng H, Lee CM, Chua GG, Pillay PK, The Brain Bench: Virtual tools for stereotactic frame neurosurgery, *Medical Image Analysis* **1**(4): 317–329, 1997.
14. Chui CK, Teo JCM, Teoh SH, Ong SH, Wang YP, Li J, Wang Z, Yan CH, Ma X, Anderson JH, Nowinski WL, A finite element spine model from VHD male data, in *Technical Abstracts of The Fourth Visible Human Conference* (17–19 October 2002, Keystone, Colorado, USA; the full paper available at http://www.uchsc.edu/sm/chs/events/vh_conf/proceedings.htm).
15. Li ZR, Chui CK, Cai YY, Amrith S, Goh PS, Anderson JH, Teo J, Liu C, Kusuma I, Siow YS, Nowinski WL, Modeling of human orbit from MR images, in *Proceedings of 5th International Conference on Medical Image Computing and Computer-assisted Intervention MICCAI 2002*, Tokyo, Japan, *Lecture Notes in Computer Science* (Springer-Verlag) **2489**(2):339–347, 2002.
16. Chen XS, Chui CK, Teoh SH, Ong SH, Nowinski WL, Automatic modeling of anatomical structures for biomedical analysis and visualization in a virtual spine workstation, in *Proceedings of 4th International Conference on Medical Image Computing and Computer-assisted Intervention MICCAI 2001*, Utrecht, The Netherlands, 14–17 October 2001, Lecture Notes in Computer Science (Springer-Verlag) **1679**:1170–1171, 2001.
17. Blacker T, Meeting the Challenge for Automated Conformal Hexahedral Meshing, in *Proceedings of 9th International Meshing Roundtable*, pp. 11–19, 2000.
18. Kessel RG, *Basic Medical Histology, The Biology of Cells, Tissues and Organs*, Oxford University Press, New York, USA, 1998.
19. Fung YC, *Foundations of Solid Mechanics*, Prentice-Hall, Englewood Cliffs, NJ, USA, 1965.
20. Miller K, Chinzei K, Orssengo G, Bednarz P, Mechanical properties of brain tissue *in vivo*: Experiment and computer simulation, *J Biomech* **33**(11):1369–1376, 2000.
21. Miller K, Chinzei K, Mechanical properties of brain tissue in tension, *J Biomech* **35**(4):483–490, 2002.
22. Miller K, Chinzei K, Constitutive modeling of brain tissue; experiment and theory, *J Biomech* **30**(11/12): 1115–1121, 1997.
23. Mow VC, Kuei SC, Lai WM, Armstrong CG, Biphasic creep and stress relaxation of articular cartilage in compression: Theory and experiments, *Trans ASME, J Biomech Engng* **102**:73–84, 1980.
24. Almeida ES, Spilker RL, Mixed and penalty finite element models for the nonlinear behaviour of biphasic soft tissues in finite deformation, *Comp Meth Biomech Biomed Eng* **1**:25–46, 1997.
25. Mow VC, Ateshian GA, Spilker RL, Biomechanics of diarthrodial joints: A review of twenty years of progress, *Trans ASME, J Biomech Eng* **115**:460–467, 1993.
26. Brown TD, Singerman RJ, Experimental determination of the linear biphasic constitutive coefficients of human fetal proximal femoral chondroepiphysis, *J Biomech* **19**:597–605, 1986.
27. Laible JP, Pflaster D, Simon BR, Krag MH, Pope M, Haugh LD, A dynamic material parameter estimation procedure for soft tissue using a poroelastic finite element model, *Trans of ASME, J Biomech Engng* **116**:19–29, 1994.
28. Nagashima T, Tamaki N, Matsumoto S, Horwitz B, Seguchi Y, Biomechanics of hydrocephalus: A new theoretical model, *Neurosurgery* **21**(6):898–903, 1987.
29. Kaczmarek M, Subramaniam RP, Neff SR, The hydromechanics of hydrocephalus: Steady-state solutions for cylindrical geometry, *Bull Math Biol* **59**(2): 295–323, 1997.

30. Peña A, Bolton MD, Whitehouse H, Pickard JD, Effects of brain ventricular shape on periventricular biomechanics: A finite-element analysis, *Neurosurgery* **45**(1): 107–118, 1999.
31. Biot MA, General theory of three dimensional consolidation, *J App Phy* **12**: 155–164, 1941.
32. Bowen RM, Theory of mixtures, in Eringen AC (ed.), *Continuum Physics*, Vol. II. Academic, New York, 1976.
33. Ozawa H, Matsumoto T, Ohashi T, Sato M, Kokubun S, Comparison of spinal cord gray matter and white matter softness: Measurement by pipette aspiration method, *J Neurosurg* **95**(2 Suppl.):221–224, 2001.
34. Nolte J, The Human Brain: An Introduction to its Functional Anatomy, Mosby-Year Book, Inc. Missouri, 1993.
35. Wang MC, Escott EJ, Breeze RE, Posterior fossa swelling and hydrocephalus resulting from hypertensive encephalopathy: Case report and review of the literature, *Neurosurgery* **44**(6):1325–1327, 1999.
36. Taylor Z, Miller K, Reassessment of brain elasticity for analysis of biomechanisms of hydrocephalus, to appear in *J Biomech*, 2003.
37. ABAQUS Theory Manual Version 5.2, Hibbit, Karlsson & Sorensen, Inc., 1998.
38. Miller K, Chinzei K, New UWA Robot — possible application to neurosurgery, *Tech Papers ISA, Biomed Sci Instrum* **36**:135–140, 2000.